# FAK is required for the assembly of podosome rosettes

Yi-Ru Pan,[1] Chien-Lin Chen,[1] and Hong-Chen Chen[1,2,3,4]

[1]Department of Life Sciences and [2]Agricultural Biotechnology Center, National Chung Hsing University, Taichung 402, Taiwan
[3]Center of infectious Disease and Signaling Research, National Cheng Kung University, Tainan 701, Taiwan
[4]Department of Nutrition, China Medical University, Taichung 404, Taiwan

Podosomes are dynamic actin-enriched membrane structures that play an important role in invasive cell motility and extracellular matrix degradation. They are often found to assemble into large rosettelike structures in highly invasive cells. However, the mechanism of this assembly remains obscure. In this study, we identified focal adhesion kinase (FAK) as a key molecule necessary for assembly. Moreover, phosphorylation of p130Cas and suppression of Rho signaling by FAK were found to be important for FAK to induce the assembly of podosome rosettes. Finally, we found that suppression of vimentin intermediate filaments by FAK facilitates the assembly of podosome rosettes. Collectively, our results strongly suggest a link between FAK, podosome rosettes, and tumor invasion and unveil a negative role for Rho signaling and vimentin filaments in podosome rosette assembly.

## Introduction

Podosomes are dynamic actin-enriched membrane structures that represent protrusions of the ventral plasma membrane and have an important role in invasive cell motility and ECM degradation (Linder, 2007). After the discovery of podosomes in fibroblasts transformed by the Rous sarcoma virus (Chen et al., 1985), similar structures have also been found in several types of normal cells, including osteoclasts, macrophages, dendritic cells, endothelial cells, and vascular smooth muscle cells (Linder and Aepfelbacher, 2003). Many invasive cancer cells display structures similar to podosomes, called invadopodia, that represent the major sites of ECM degradation in these cells. The current convention is to use the term podosome for the structures found in normal cells and Src-transformed cells and to call the structures found in invasive cancer cells invadopodia (Gimona et al., 2008).

Podosomes are dot-shaped structures with a diameter of 0.5–1 µm and a height of 0.2–5 µm, composed of a core of F-actin and actin regulators, such as cortactin and the Arp2/3 complex, and surrounded by a ring structure containing integrins, scaffolding proteins, and kinases (Linder and Aepfelbacher, 2003). They are found either isolated both in macrophages and dendritic cells or arranged into superstructures in osteoclasts and other types of cells. In Src-transformed fibroblasts, podosomes are often organized into large rosette-shaped structures with a diameter of 5–20 µm. Such podosome rosettes can also be found in osteoclasts (Destaing et al., 2003), endothelial cells (Tatin et al., 2006), and some highly invasive cancer cells (Kocher et al., 2009). In particular, osteoclasts seeded on glass develop podosomes that are first grouped into clusters, which assemble into small podosome rings (or rosettes) and eventually into a large beltlike structure at the cell periphery (Destaing et al., 2003). When seeded on bone or a bonelike substrate, osteoclasts develop a large and dense F-actin ring, called the sealing zone, where osteoclasts secrete protons and proteases to dissolve and degrade the mineralized matrix (Luxenburg et al., 2007). Therefore, podosomes can serve as the structural unit for superstructures such as podosome rosettes or belts. However, the mechanism of the organization of podosomes into such superstructures remains obscure.

Focal adhesion kinase (FAK), a 125-kD nonreceptor tyrosine kinase localized in focal adhesions, is known for its pivotal role in the control of a variety of cell functions (McLean et al., 2005). FAK was originally identified as a substrate of Src and was subsequently found to be activated upon cell adhesion to ECM proteins (Guan and Shalloway, 1992) as well as by some

Correspondence to Hong-Chen Chen: hcchen@nchu.edu.tw

Abbreviations used in this paper: FAK, focal adhesion kinase; HUVEC, human umbilical vein endothelial cell; MEF, mouse embryo fibroblast; MMP, matrix metalloproteinase; RANKL, receptor activator of NFkB ligand; ROCK, Rho-associated kinase; SH, Src homology; shRNA, small hairpin RNA; TAT, transactivator of transcription; t-TA, tetracycline-controlled transactivator; wt, wild type.
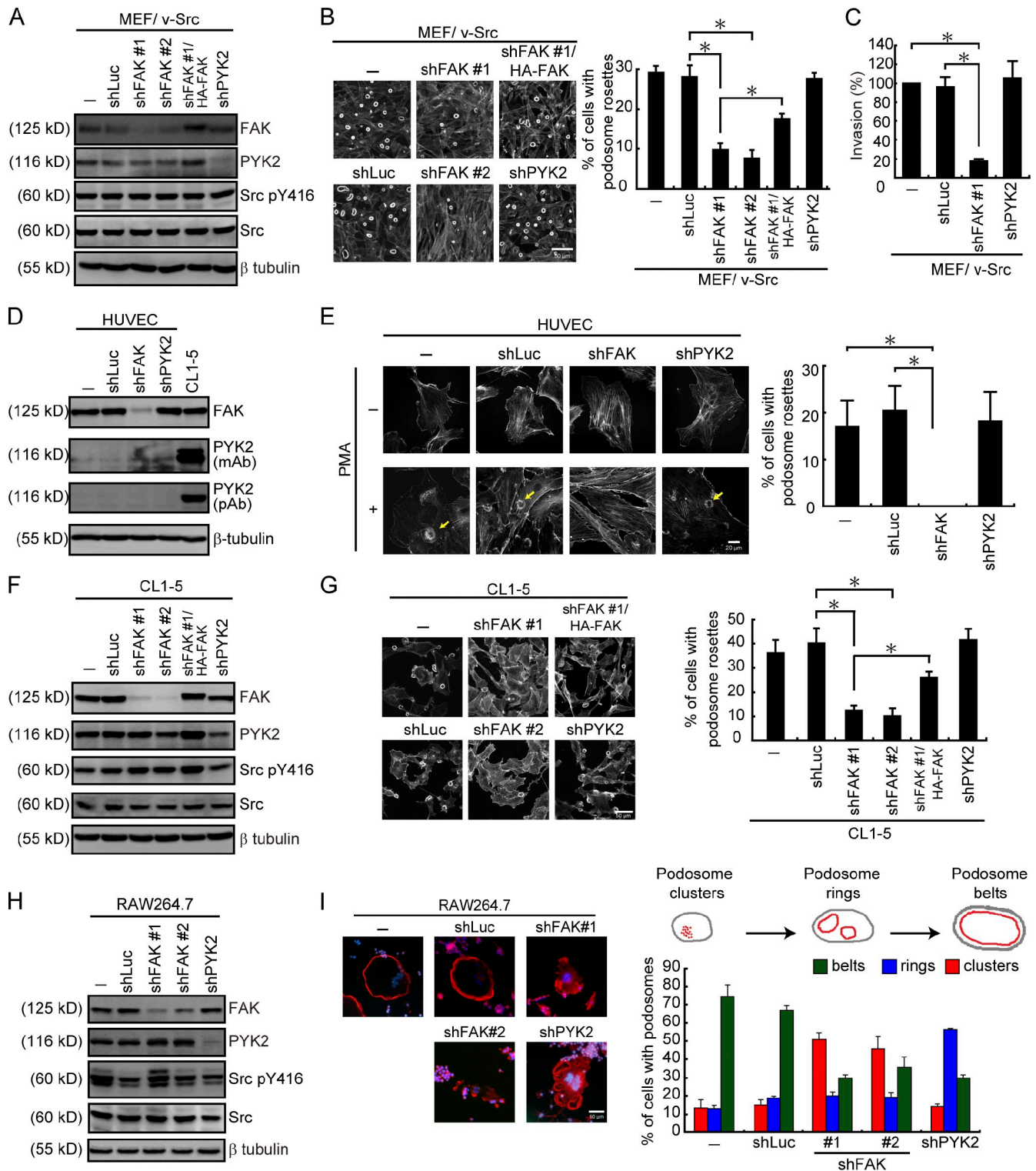
THE JOURNAL OF CELL BIOLOGY

Figure 1. **FAK is crucial for podosome rosette assembly in various types of cells.** (A) shRNAs specific to FAK (shFAK; clones #1 and #2), PYK2 (shPYK2), or luciferase (shLuc) were stably expressed in v-Src–transformed MEFs. HA-FAK resistant to shFAK was reexpressed into the cells expressing shFAK#1 (shFAK#1/HA-FAK). An equal amount of whole-cell lysates was analyzed by immunoblotting with the indicated antibodies. (B) The cells were stained for F-actin. The percentage of the cells containing podosome rosettes in the total counted cells ($n \geq 300$) was determined. (C) The cells were subjected to a Matrigel invasion assay. Data were quantified and expressed as a percentage relative to the level of the control. (D) HUVECs and those expressing shRNAs were analyzed by immunoblotting. A monoclonal anti-PYK2 (mAb) and a polyclonal anti-PYK2 (pAb) were used to detect PYK2. (E) The cells were treated with (+) or without (−) 100 nM PMA for 3 h and stained for F-actin. Arrows indicate podosome rosettes. The percentage of the cells containing podosome rosettes in the total counted cells ($n \geq 300$) was determined. (F) shRNAs specific to FAK (clones #1 and #2), PYK2, or luciferase were stably expressed in CL1-5 cells. HA-FAK resistant to shFAK was reexpressed into the cells expressing shFAK #1. Whole-cell lysates were analyzed by immunoblotting with the indicated antibodies. (G) The cells were stained for F-actin, and the percentage of the cells containing podosome rosettes in the total counted cells ($n \geq 300$) was determined. (H) Cell lysates from RAW264.7 cells and those expressing shRNAs were analyzed by immunoblotting with the indicated antibodies.

growth factors (Sieg et al., 2000; Chen and Chen, 2006). Y397 is the major site of FAK autophosphorylation, which creates a high-affinity binding site for the Src homology (SH) 2 domain of several proteins including the Src family kinases (Schaller et al., 1994). Activated Src phosphorylates FAK on multiple sites including Y576 and Y577, both of which are located in the activation loop within the kinase domain (Calalb et al., 1995). The ensuing phosphorylation of FAK on Y576 and Y577 is required for the full enzymatic activity of FAK. Fibroblasts derived from FAK-null (FAK$^{-/-}$) mouse embryos are more rounded and poorly spread than their wild-type (wt) counterparts (Ilić et al., 1995). They show an overabundance of focal adhesions, enriched cortical actin filaments at the cell periphery, and a decreased migration rate. It has been shown that an increase in peripheral adhesions results from an inhibition of turnover in FAK$^{-/-}$ cells, which may be attributed to constitutive activation of RhoA and Rho-associated kinase (ROCK; Ren et al., 2000; Chen et al., 2002).

Increased expression and tyrosine phosphorylation of FAK have been correlated with the progression to an invasive cell phenotype (Schlaepfer et al., 2004). Given its close relationship with integrins, focal adhesion proteins, and actin regulators, it is generally believed that FAK plays an important role in podosomes/invadopodia. However, some recent studies do not appear to support this assumption (Vitale et al., 2008; Chan et al., 2009), claiming that although FAK is important for cell invasion, it is not required for the formation of invadopodia in cancer cells. In this study, we demonstrate that although FAK is dispensable for dot-shaped podosomes, it is required for the assembly of podosome rosettes. Additionally, our results show that the induction of podosome rosettes by FAK promotes matrix degradation and cell invasion, supporting a role of FAK in malignant tumor progression. We propose that FAK may regulate podosome rosettes through its effect on p130Cas phosphorylation, Rho signaling, and vimentin intermediate filaments.

# Results

### FAK, but not PYK2, is crucial for the formation of podosome rosettes in fibroblasts, endothelial cells, and carcinoma cells

We first examined whether FAK plays a role in the formation of podosome rosettes in Src-transformed fibroblasts. Depletion of FAK, but not the other FAK family member PYK2, significantly suppressed podosome rosette formation and Matrigel invasion in Src-transformed mouse embryo fibroblasts (MEFs; Figs. 1 [A–C] and S1) and Src-transformed NIH3T3 cells (Fig. S2). In human umbilical vein endothelial cells (HUVECs), PYK2 was hardly detected (Fig. 1 D). Knockdown of FAK completely suppressed PMA-induced formation of podosome rosettes in HUVECs (Fig. 1 E). In lung carcinoma CL1-5 cells, depletion of FAK, but not PYK2, led to a decreased formation of rosettelike structures in the cells (Fig. 1, F and G). These structures are truly podosome

rosettes because they are exclusively found at the ventral aspect of the cell and serve as the sites for the cell to degrade underlying matrix proteins (Fig. S2 C). Collectively, our results indicate that FAK, but not PYK2, is crucial for podosome rosette formation in fibroblasts, endothelial cells, and carcinoma cells.

### FAK and PYK2 may regulate different patterning of podosomal organization in osteoclasts

Mouse RAW264.7 cells can differentiate into osteoclast-like cells by receptor activator of NFκB ligand (RANKL; Boyle et al., 2003). After induction by RANKL, RAW264.7 cells became multinucleated, and their podosomes were mainly organized into a large beltlike structure at the cell periphery (Fig. 1, H and I). However, FAK depletion in RAW264.7 cells impaired this process, keeping podosomes as clusters in the cells (Fig. 1 I). PYK2 depletion also had an adverse effect on the formation of podosome belts in differentiated RAW264.7 cells, which led to podosome rings being the major type of podosome structures in the cells (Fig. 1, H and I). These results suggest that in osteoclasts, FAK may be essential for the cluster-to-ring transition of podosomes, whereas PYK2 may be crucial for the ring-to-belt transition of podosomes.

### FAK is dispensable for dot-shaped podosomes but is essential for assembly into rosette-shaped structures

To examine the necessity of FAK in the assembly of podosome rosettes, FAK$^{-/-}$ MEFs and their wt counterparts (FAK$^{+/+}$) were used in this study (Fig. 2 A). Before transformation by v-Src, both FAK$^{+/+}$ and FAK$^{-/-}$ MEFs had almost no podosomes (Fig. 2 B). Strikingly, v-Src induced podosome rosettes only in FAK$^{+/+}$ MEFs but not in FAK$^{-/-}$ MEFs (Fig. 2 B). However, v-Src induced small dot-shaped podosomes in both FAK$^{+/+}$ and FAK$^{-/-}$ MEFs to a similar extent (Fig. 2, B–D). These results suggest that although FAK is dispensable for dot-shaped podosomes, it is essential for the assembly of podosome rosettes. Moreover, the formation of podosome rosettes in v-Src–transformed FAK$^{+/+}$ MEFs was correlated with increases in ECM degradation (Fig. 2 E) and Matrigel invasion (Fig. 2 F). The increased invasiveness of v-Src–transformed FAK$^{+/+}$ MEFs was not because of an increase in matrix metalloproteinases (MMPs; Fig. 2 G).

### Elevated expression of FAK is correlated with increases in podosome rosette formation, matrix degradation, and invasion

To further examine the necessity of FAK for the assembly of podosome rosettes, an inducible (Tet-Off) FAK expression system was established in v-Src–transformed FAK$^{-/-}$ MEFs (Fig. 3 A). As described in Fig. 2, dot-shaped podosomes were already present in v-Src–transformed FAK$^{-/-}$ MEFs before FAK induction. Only upon FAK expression were podosome rosettes allowed to assemble. The extent of podosome rosette

(I) The cells were treated with 100 ng/ml GST-RANKL for 7 d and stained for F-actin and nuclei. Cells containing more than three nuclei were defined as osteoclasts. The percentage of the osteoclasts containing podosome clusters, rings, or belts in the total counted osteoclasts ($n \geq 100$) was determined. (B, C, E, G, and I) Values (means ± SD) are from three independent experiments. *, P < 0.005.
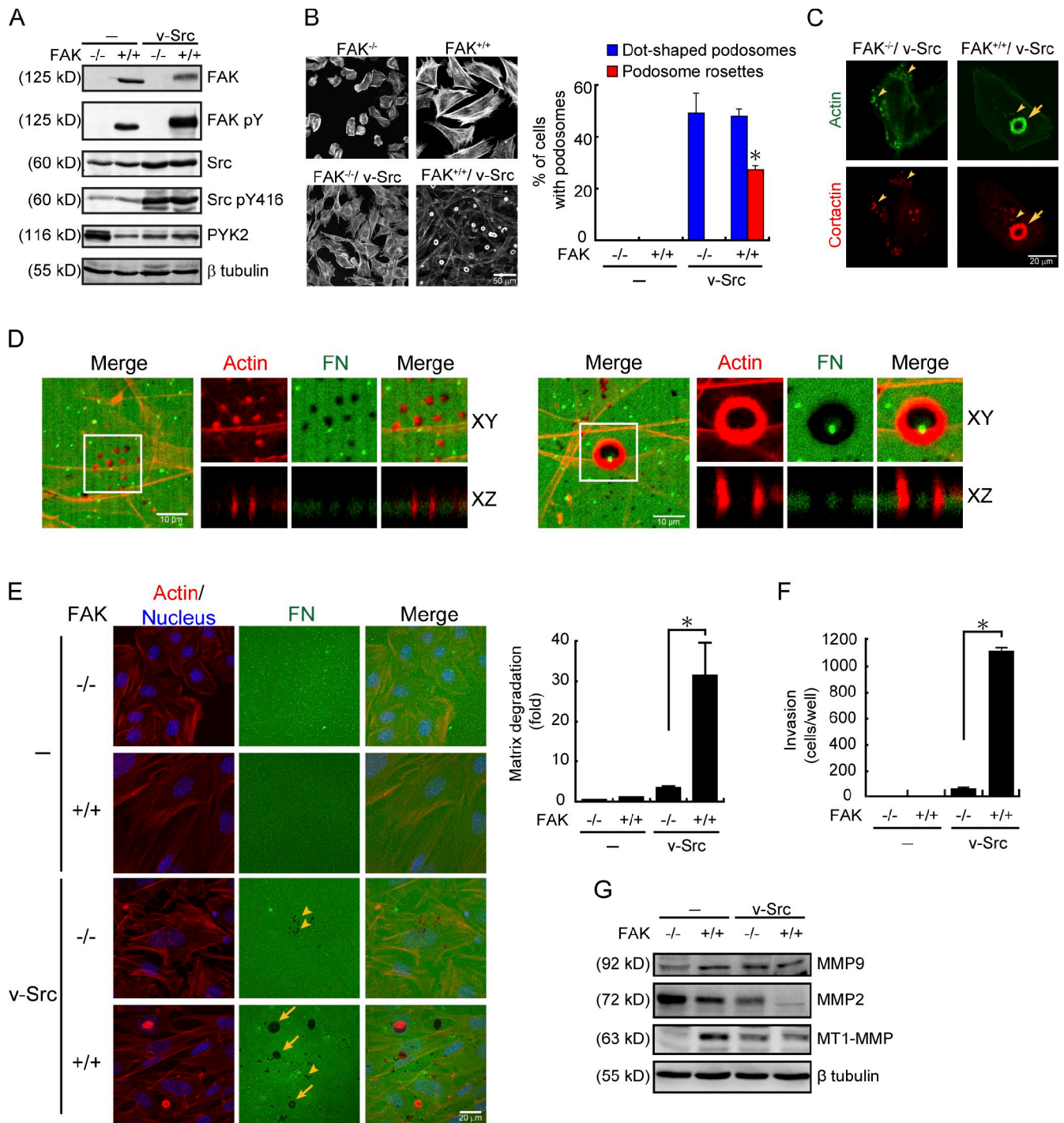
Figure 2. **FAK is dispensable for the formation of dot-shaped podosomes but is essential for the assembly of podosome rosettes.** (A) Whole-cell lysates from FAK+/+ MEFs, FAK−/− MEFs, and those transformed by v-Src were analyzed by immunoblotting with the indicated antibodies. (B) The percentage of the cells with dot-shaped podosomes and podosome rosettes in the total counted cells ($n \geq 300$) was determined. (C) The cells were stained for F-actin and cortactin. Representative high-power images are shown. Arrows indicate podosome rosettes. Arrowheads indicate dot-shaped podosomes. (D) v-Src–transformed MEFs were seeded on Alexa Fluor 488–conjugated fibronectin (FN) for 24 h and then stained for F-actin. The z stack images were obtained and reconstituted by confocal microscopy. The XY and XZ sections of the boxed areas are shown. Left, dot-shaped podosomes; right, podosome rosettes. (E) The cells were seeded on Alexa Fluor 488–conjugated fibronectin for 24 h and then stained for F-actin and nuclei. Arrowheads indicate the areas in which fibronectin was degraded by dot-shaped podosomes. Arrows indicate the areas in which fibronectin was degraded by podosome rosettes. The areas in which fibronectin had been degraded were measured and expressed as fold relative to the level of FAK+/+ MEFs. (F) Matrigel invasion assay. (B, E, and F) Values (means ± SD) are from three independent experiments. *, $P < 0.005$. (G) An equal amount of whole-cell lysates was analyzed for MMP expression by immunoblotting.
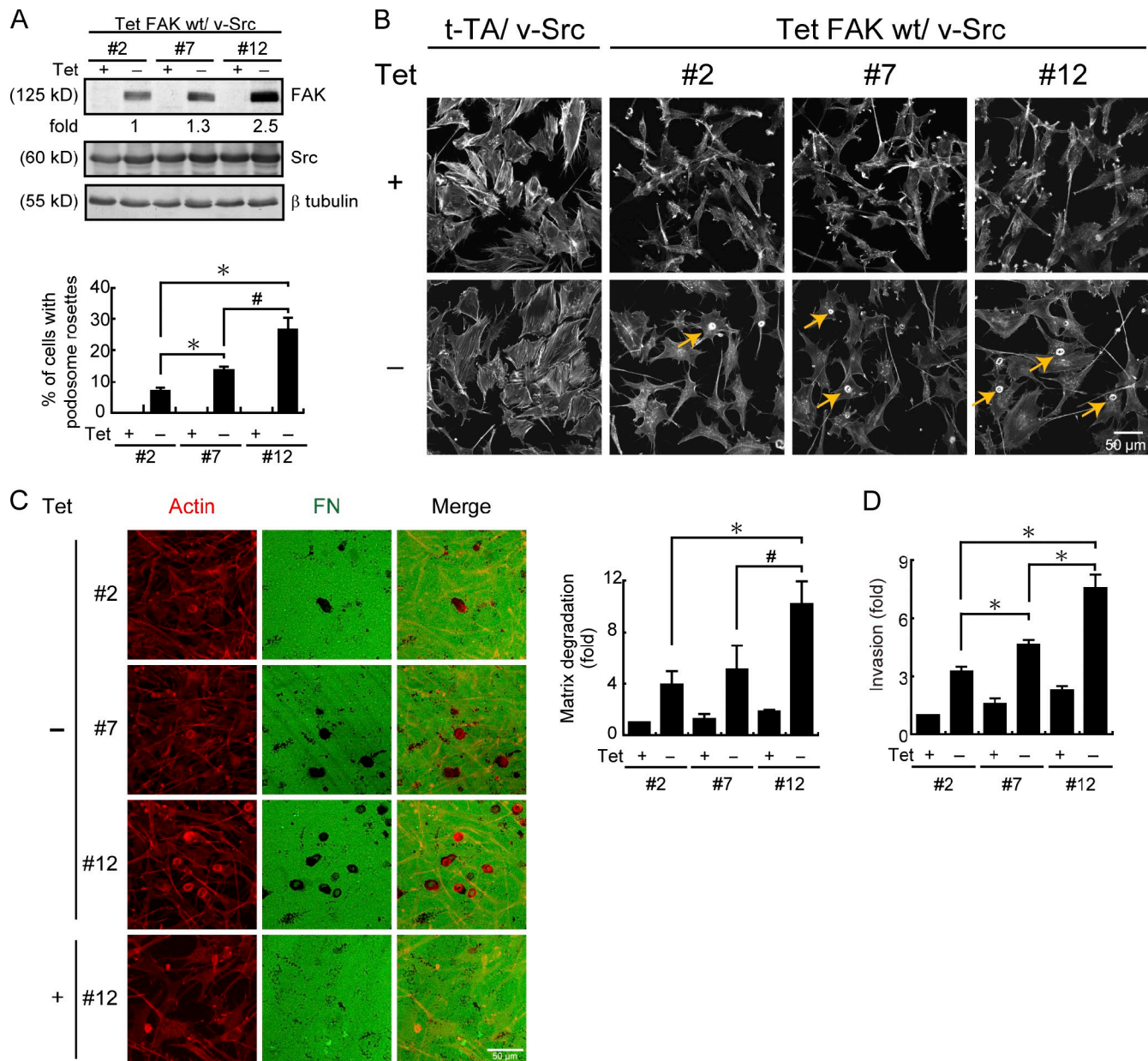
Figure 3.  **Increased expression of FAK is correlated with increases in podosome rosette formation, matrix degradation, and cell invasion.** (A) An inducible (Tet-Off) expression system for wt FAK expression was established in v-Src–transformed FAK$^{-/-}$ MEFs (Tet FAK wt/v-Src). Three cell clones (#2, #7, and #12) were selected and maintained in the medium with (+) tetracycline. The cells were allowed to express FAK upon tetracycline withdrawal (−). 24 h after tetracycline withdrawal, FAK expression was analyzed by immunoblotting. The expression level of FAK was quantified and expressed as fold relative to the level of clone #2. (B) Three FAK-inducible clones and a control clone (tetracycline-controlled transactivator [t-TA]) that encodes t-TA were grown in the medium with or without tetracycline for 24 h and were then stained for F-actin. Arrows indicate podosome rosettes. The percentage of the cells containing podosome rosettes in the total counted cells ($n \geq 300$) was determined. #, $P < 0.05$. (C) The cells were grown in the medium with or without tetracycline for 24 h and were plated on Alexa Fluor 488–conjugated fibronectin (FN) for another 24 h. The areas in which fibronectin was degraded were measured and expressed as fold relative to the area degraded by clone #2 in the presence of tetracycline. #, $P < 0.05$. (D) The cells were grown in the medium with or without tetracycline for 24 h and were then subjected to a Matrigel invasion assay. Data were quantified and expressed as fold relative to the level of clone #2 in the presence of tetracycline. (B–D) Values (means ± SD) are from at least three independent experiments. *, $P < 0.005$.

formation was correlated with the expression level of FAK (Fig. 3 B). Moreover, the increase in podosome rosettes was correlated with increases in ECM degradation (Fig. 3 C) and invasion (Fig. 3 D). Together, these results suggest that increased expression of FAK may contribute to v-Src–induced cell invasion, at least in part, through its effect on the induction of podosome rosette assembly.

**FAK is localized to podosome rosettes and some dot-shaped podosomes**

Confocal microscopic analysis revealed that FAK is colocalized with active Src at podosome rosettes in v-Src–transformed MEFs (Fig. 4, A and B). Like endogenous FAK, GFP-fused FAK (GFP-FAK) was found to localize to podosome rosettes. Notably, the COOH domain (aa 687–1,053), but not the NH2
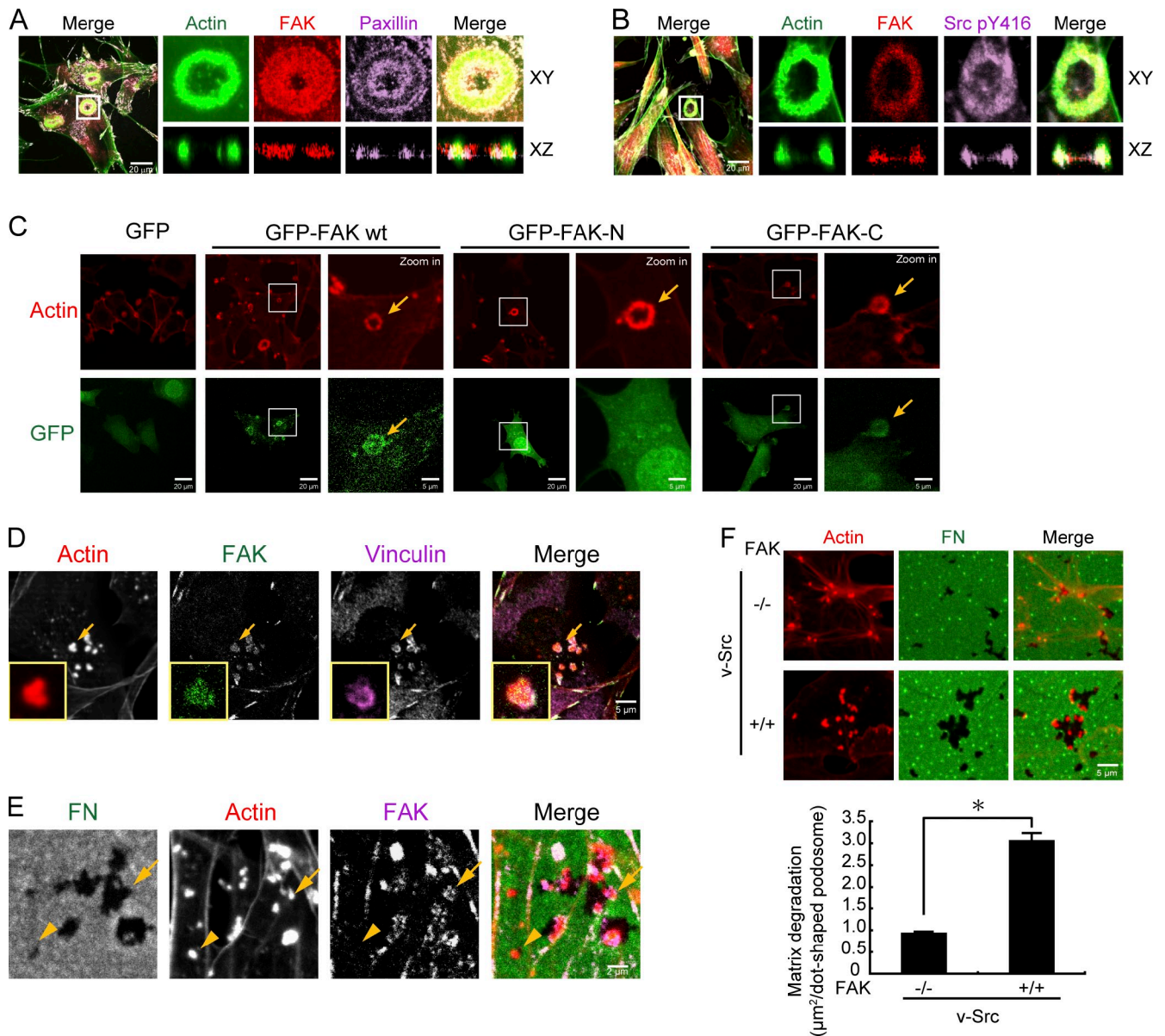
Figure 4. **FAK is localized to podosome rosettes and some dot-shaped podosomes.** (A and B) v-Src–transformed FAK^{+/+} MEFs were fixed and stained for F-actin, FAK, paxillin, and active Src (Src pY416). The z stack images were obtained and reconstituted by confocal microscopy. The XY and XZ sections of the boxed areas containing a podosome rosette are shown. (C) GFP, GFP-FAK, GFP-FAK-NH2 (GFP-FAK-N) domain, or GFP-FAK-COOH (GFP-FAK-C) domain was transiently expressed in Src-transformed 3T3 cells and then stained for F-actin. Arrows indicate podosome rosettes. Note that the GFP-FAK-NH2 domain is not localized to podosome rosettes. (D) v-Src–transformed MEFs were stained for F-actin, vinculin, and FAK. The representative image shows that FAK and vinculin are localized to dot-shaped podosomes. Arrows indicate dot-shaped podosomes that are enlarged and shown in the insets. (E) v-Src–transformed FAK^{+/+} MEFs were seeded on Alexa Fluor 488–conjugated fibronectin (FN) for 24 h and then stained for F-actin and FAK. Arrowheads indicate dot-shaped podosomes without FAK association. Arrows indicate dot-shaped podosomes with FAK association. Note that dot-shaped podosomes with FAK association have higher matrix-degrading activity than those without FAK association. (F) The cells were seeded on labeled fibronectin for 24 h. The mean degraded area by a dot-shaped podosome was measured ($n = 15$). Values (means ± SD) are from three independent experiments. *, $P < 0.005$.

domain (aa 1–391), of FAK was localized to podosome rosettes (Fig. 4 C), indicating that the COOH domain of FAK is responsible for its targeting to podosome rosettes.

As described in other types of cells, each podosome has an F-actin core surrounded by focal adhesion proteins such as vinculin (Fig. 4 D). Notably, FAK was found to associate with some, but not all, dot-shaped podosomes (Fig. 4, E and F). The dot-shaped podosomes with FAK association were more potent than those without FAK association in the degradation of ECM proteins (Fig. 4, E and F). Together, these results

indicate that although FAK is dispensable for the formation of dot-shaped podosomes, it is important for their matrix-degrading activity.

### The Y397 and catalytic activity of FAK are essential for the triggering of podosome rosette assembly

To examine whether the autophosphorylation site Y397 and catalytic activity of FAK are required for the induction of podosome rosettes, an inducible (Tet-Off) expression for Y397F and

Y566F/Y577F mutants was established in v-Src–transformed FAK$^{-/-}$ MEFs. Although the expression levels of both mutants were threefold higher than wt FAK (Fig. 5 A), they hardly induced podosome rosettes (Fig. 5 B), indicating that the Y397 and catalytic activity of FAK are required for triggering the assembly of podosome rosettes.

Moreover, the FAK ΔC mutant with a deletion (aa 687–1,053) at its COOH domain was defective in inducing podosome rosettes in v-Src–transformed FAK$^{-/-}$ MEFs (Fig. 5 E). In contrast, the FAK ΔN mutant with a deletion (aa 1–375) at its NH2 domain was more potent than wt FAK in inducing podosome rosettes (Fig. 5 E). The increased capability of the ΔN mutant to induce podosome rosettes could be attributed to its increased catalytic activity (Fig. 5 F). We have previously demonstrated that substitution of FAK at Tyr194 with Glu leads to FAK activation (Chen et al., 2011). The Y194E mutant significantly increased the formation of podosome rosettes in CL1-5 cells (Fig. 5, G and H). However, this increase was suppressed by the Src-specific inhibitor PP2 (Fig. 5 H), indicating that the activity of Src is required for FAK to induce the assembly of podosome rosettes.

### Interaction of FAK with p130Cas is important for podosome rosette formation

To examine the mechanisms of induction of podosome rosettes by FAK, FLAG epitope–tagged FAK and its various mutants were stably reexpressed in v-Src–transformed FAK$^{-/-}$ MEFs (Fig. 6 A), and their ability to induce podosome rosettes in those cells was measured (Fig. 6 B). Consistent with the results shown in Fig. 5, the Y397F mutant was deficient in inducing podosome rosettes in v-Src–transformed FAK$^{-/-}$ MEFs (Fig. 6 B). The K454R mutant that is defective in ATP binding and thereby has a decreased kinase activity was deficient in inducing podosome rosettes (Fig. 6 B). Notably, the P712A/P715A mutant defective in p130Cas binding (Cary et al., 1998) had an impaired capability to induce podosome rosettes (Fig. 6 B), thus suggesting that interaction of FAK with p130Cas may be crucial for podosome rosette assembly. Accordingly, the tyrosine phosphorylation of p130Cas, but not cortactin and Tks5, was correlated with the expression of FAK in Src-transformed MEFs (Fig. 6 C).

The significance of p130Cas expression in podosome rosettes was demonstrated by a knockdown approach (Fig. 6, D and E). However, the constitutively active Y194E mutant of FAK hardly induced p130Cas phosphorylation in SYF (src$^{-/-}$ yes$^{-/-}$ fyn$^{-/-}$) cells (Fig. 6 F), suggesting that FAK may not be the kinase directly phosphorylating p130Cas. Instead, FAK may function as a docking protein for Src to phosphorylate p130Cas. Consistent with this notion, the p130Cas SH3 domain that interferes with the interaction between FAK and p130Cas (Cary et al., 1998) partially suppressed podosome rosettes in Src-transformed 3T3 cells (Fig. 6 G).

### Suppression of Rho signaling by FAK is crucial for podosome rosette assembly

FAK has been reported to suppress Rho activity (Ren et al., 2000; Chen et al., 2002). Indeed, the activity of Rho, but not Rac and Cdc42, was inversely correlated with the expression of FAK (Fig. 7 A). Membrane-permeable active Rho

(transactivator of transcription [TAT]–RhoV14) decreased the formation of podosome rosettes in v-Src–transformed MEFs (Fig. 7 B). In contrast, membrane-permeable C3 exoenzyme (TAT-C3), which specifically ADP ribosylates and inactivates Rho, rescued the defect in the podosome rosette formation caused by FAK depletion (Fig. 7 B). Thus, FAK may promote podosome rosette formation, at least in part, through its suppression of Rho activity. Indeed, p190RhoGAP was colocalized with FAK at podosome rosettes (Fig. 7 C) and was important for the formation of podosome rosettes (Fig. 7 D). Intriguingly, knockdown of p130Cas increased the Rho activity (Fig. 7 E), suggesting a potential role of p130Cas in Rho inhibition.

Moreover, inhibition of ROCK by the inhibitor Y27632 apparently enhanced the formation of dot-shaped podosomes, but not podosome rosettes, in v-Src–transformed FAK$^{-/-}$ MEFs (Fig. 8, A and B). In contrast, Y27632 significantly promoted the formation of podosome rosettes in v-Src–transformed FAK$^{+/+}$ MEFs (Fig. 8 A), correlating with increases in matrix degradation (Fig. 8 C) and Matrigel invasion (Fig. 8 D). These results not only support that hyperactivation of Rho and ROCK antagonizes the formation of podosome rosettes but also provide an example to show that increased numbers of dot-shaped podosomes do not spontaneously trigger the assembly of podosome rosettes in the absence of FAK.

Podosome rosettes are dynamic structures with a life span of minutes to hours. The formation of podosome rosettes can be divided into three phases: assembly, maintenance, and disassembly (Fig. 8 E). FAK was found to associate with podosomes in the early assembly phase and then throughout the process (Fig. 8 E). Interestingly, the disassembly of podosome rosettes is always manifested by collapse of the F-actin ring structure toward its center before it is completely dissolved (Fig. 8 E). Y27632 significantly delayed the disassembly phase (Fig. 8 F), suggesting that ROCK may facilitate the disassembly of podosome rosettes.

### Microtubule is not necessary for the formation of podosome rosettes in Src-transformed fibroblasts

Microtubule acetylation has been suggested to be important for the formation of podosome belts in osteoclasts (Destaing et al., 2005; Gil-Henn et al., 2007). In particular, in PYK2-null osteoclasts, Rho activity was increased, whereas microtubule acetylation and stability were reduced (Gil-Henn et al., 2007). This raises the possibility that FAK might promote podosome rosettes via regulation of microtubule acetylation. However, we found that although microtubule acetylation was apparently reduced in FAK-null MEFs (Fig. S3 A), it was not affected by FAK expression and was not correlated with the formation of podosome rosettes in Src-transformed MEFs (Fig. S3, B and C). Additionally, we demonstrated that the integrity of microtubules is not necessary for podosome rosette formation in Src-transformed MEFs (Fig. S3 D). Thus, it is possible that microtubule acetylation may only be involved in the ring-to-belt transition of podosomal organization in osteoclasts. This could also explain why PYK2 is essential for the formation of podosome belts, but not podosome rings, in osteoclasts (Fig. 1 I).
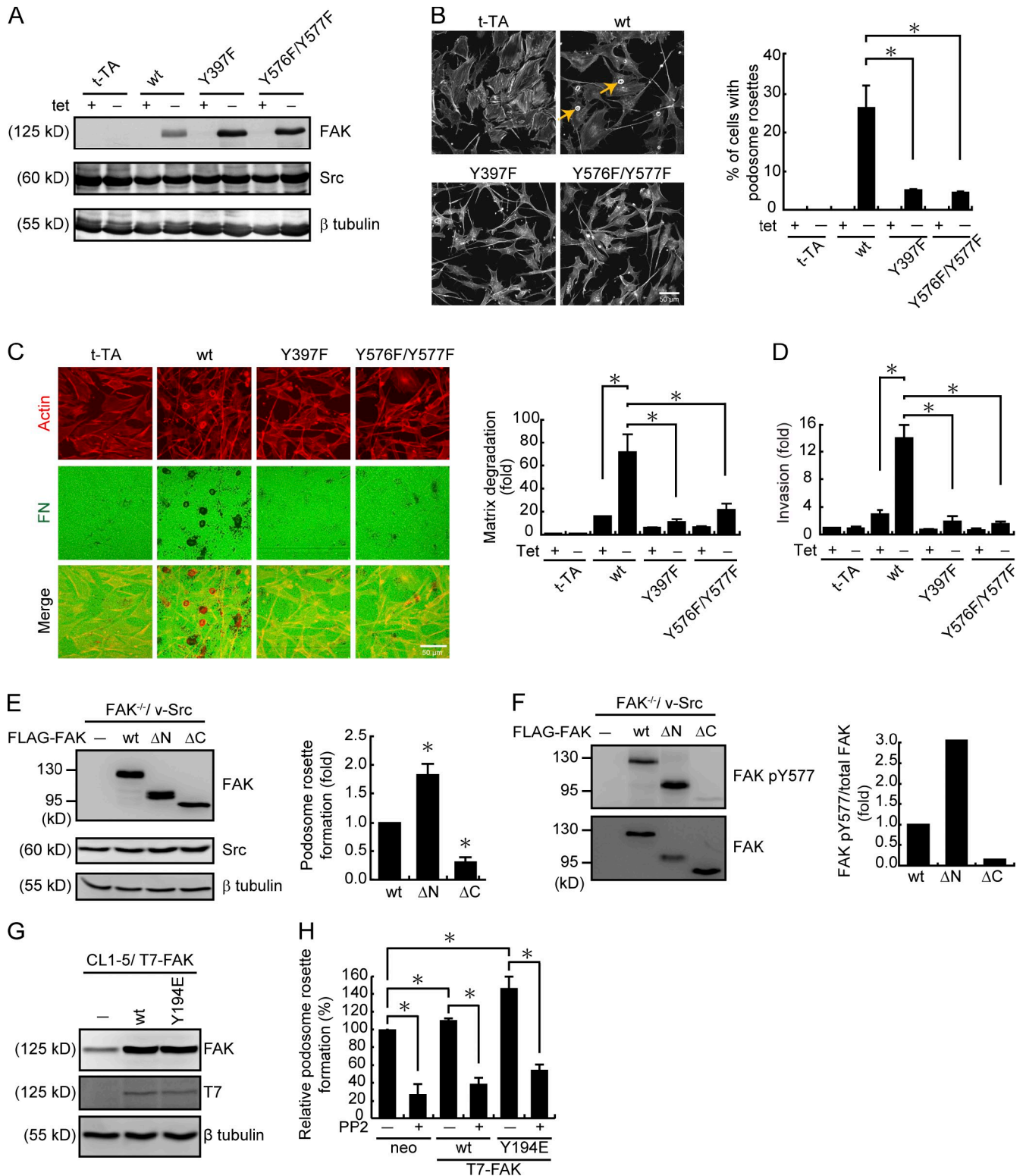
Figure 5. **The Tyr-397 and catalytic activity of FAK are essential for the triggering of podosome rosette assembly.** (A) An inducible (Tet-Off) expression system for FAK and its mutants was established in v-Src–transformed FAK$^{-/-}$ MEFs. The cells were maintained in the medium with (+) tetracycline. 24 h after tetracycline withdrawal (−), the cells were lysed and analyzed by immunoblotting. (B) The cells were grown in the absence of tetracycline for 24 h and stained for F-actin. Arrows indicate podosome rosettes. The percentage of the cells containing podosome rosettes in the total counted cells ($n \geq 300$) was determined. (C) The cells were grown in the presence or absence of tetracycline for 24 h and were then subjected to a matrix degradation assay in the presence of tetracycline. Data were quantified and expressed as fold relative to the level of the t-TA clone in the presence of tetracycline. (D) The cells were grown in the presence or absence of tetracycline for 24 h and were then subjected to a Matrigel invasion assay. Data were quantified and expressed as fold relative to the level of the t-TA clone in the presence of tetracycline. (E) FLAG-FAK or its mutants with deletion at the NH2 domain (ΔN) or the COOH domain (ΔC) were stably expressed in v-Src–transformed FAK$^{-/-}$ MEFs. An equal amount of whole-cell lysates was analyzed by immunoblotting with the indicated antibodies. The formation of podosome rosettes was quantified and expressed as fold relative to that of the cells expressing FLAG-FAK wt.
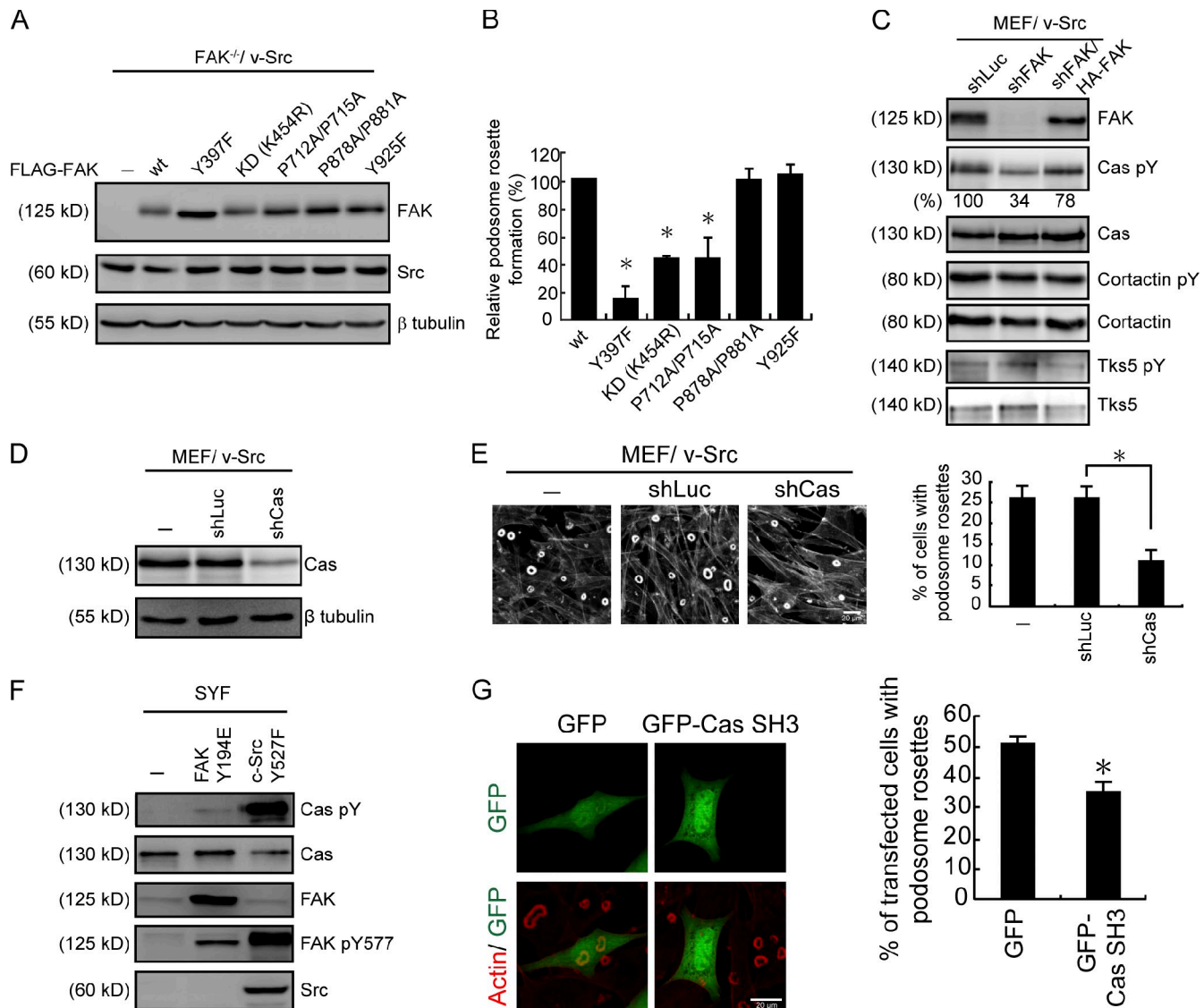
Figure 6. **Interaction of FAK with p130Cas is important for podosome rosette formation.** (A) Stable expression of FLAG-FAK and its mutants in v-Src–transformed FAK$^{-/-}$ MEFs. KD, kinase-dead mutant. (B) The formation of podosome rosettes was quantified and expressed as a percentage relative to the cells expressing FLAG-FAK wt. (C) FAK was depleted in v-Src–transformed FAK$^{+/+}$ MEFs by shRNA (shFAK). Subsequently, HA-FAK resistant to shFAK was stably reexpressed into the FAK-depleted cells (shFAK/HA-FAK). The tyrosine phosphorylation of p130Cas (Cas), cortactin, and Tks5 was analyzed. The tyrosine phosphorylation of p130Cas was quantified and expressed as a percentage relative to the level in the cells expressing shLuc. The results shown are representative of three experiments. (D) Immunoblotting for the p130Cas expression in v-Src–transformed MEFs and those expressing shRNAs specific to p130Cas (shCas) or luciferase (shLuc) as a control. (E) The cells were stained for F-actin, and the percentage of the cells containing podosome rosettes in the total counted cells ($n \geq 300$) was determined. (F) T7-FAK Y194E or c-SrcY527F was transiently expressed in SYF cells, and the tyrosine phosphorylation of p130Cas (Cas pY) was analyzed. (G) GFP or GFP-p130Cas SH3 domain (GFP-Cas SH3) was transiently expressed in Src-transformed 3T3 cells. The cells were stained for F-actin, and the percentage of the cells containing podosome rosettes in the total counted cells expressing GFP or GFP-Cas SH3 ($n \geq 100$) was determined. (B, E, and G) Values (means ± SD) are from three independent experiments. *, $P < 0.005$.

## Suppression of vimentin filaments by FAK facilitates the assembly of podosome rosettes

ROCK has been implicated to phosphorylate and regulate the organization of the intermediate filaments (Inada et al., 1999). We found that FAK depletion or TAT-RhoV14 addition apparently promoted the organization of the vimentin filaments in CL1-5 cells (Fig. 9 A), concomitant with decreased formation of podosome rosettes (Fig. 9 C). Notably, in the control CL1-5 cells, the vimentin filaments were enriched at the central region of the cells but were sparse at the cell periphery and the surrounding areas of podosome rosettes (Fig. 9 A). However, the enhanced structure of the vimentin filaments by FAK depletion or TAT-RhoV14 addition extended to the cell periphery
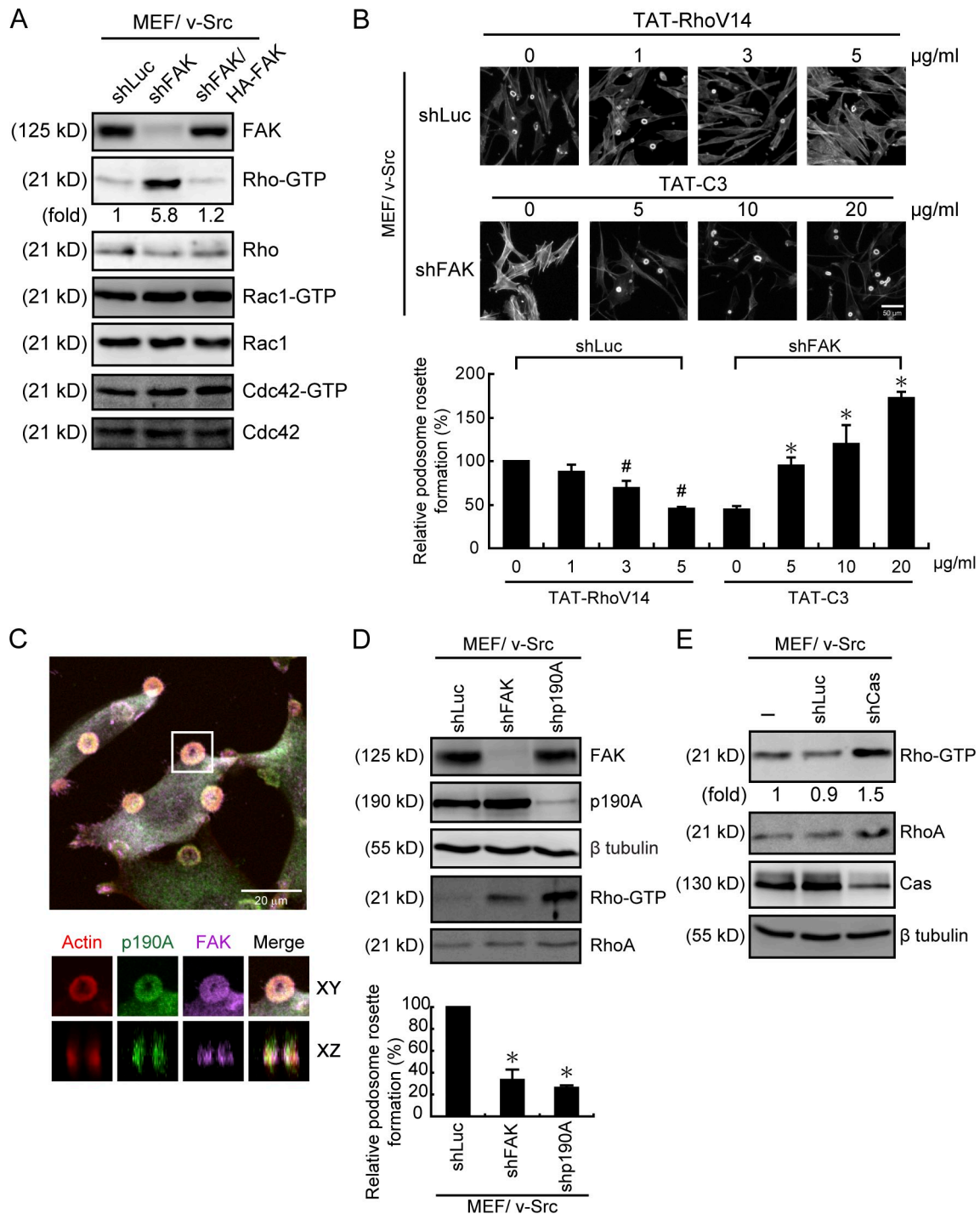
Figure 7. **Suppression of Rho signaling by FAK is crucial for podosome rosette assembly.** (A) The levels of active (GTP-bound) Rho family proteins including RhoA, Rac1, and Cdc42 in the cells were measured. The results shown are representative of three experiments. (B) v-Src–transformed MEFs expressing shRNA to luciferase (shLuc) were treated with TAT-RhoV14 at various concentrations for 12 h. v-Src–transformed MEFs expressing shRNA to FAK (shFAK) were treated with TAT-C3 at various concentrations for 12 h. The formation of podosome rosettes was measured and expressed as a percentage relative to that of control cells expressing shLuc. *, P < 0.005 (compared with the shFAK cells without TAT-C3 treatment); #, P < 0.005 (compared with the shLuc cells without TAT-RhoV14 treatment). (C) Src-transformed 3T3 cells were stained for F-actin, p190RhoGAP (p190A), and FAK. The z stack images were obtained and reconstituted by confocal microscopy. The XY and XZ sections of the boxed area containing a podosome rosette are shown. (D) v-Src–transformed MEFs and those expressing shRNAs specific to FAK, p190RhoGAP (shp190A), or luciferase were analyzed for the expression of FAK and p190RhoGAP by immunoblotting. The level of active RhoA was measured. The formation of podosome rosettes was measured and expressed as a percentage relative to that of the control cells expressing shLuc. *, P < 0.005. (B and D) Values (means ± SD) are from three independent experiments. (E) The effect of p130Cas knockdown on Rho activity was analyzed. The level of active RhoA was measured, quantified, and expressed as fold relative to the control cells. The results shown are the representative of three experiments.
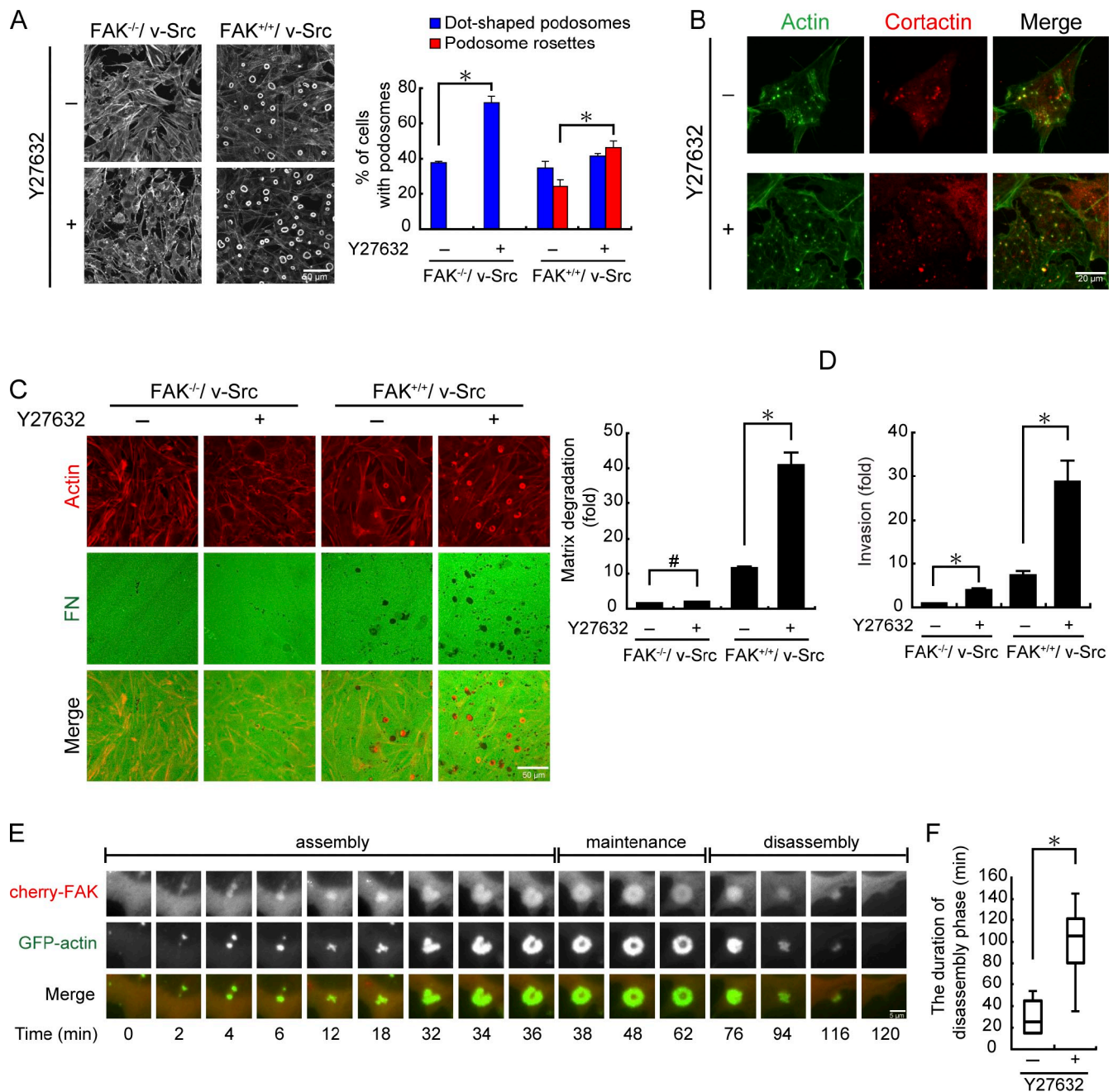
Figure 8. **ROCK facilitates the disassembly of podosome rosettes.** (A) v-Src–transformed FAK$^{-/-}$ and FAK$^{+/+}$ MEFs were treated with (+) or without (−) the ROCK inhibitor Y27632 (10 µM) for 2 h. The percentage of the cells containing dot-shaped podosomes or podosome rosettes in the total counted cells ($n \geq 300$) was determined. (B) v-Src–transformed FAK$^{-/-}$ MEFs were treated with or without 10 µM Y27632 for 2 h and stained for F-actin and cortactin. Representative high-power images are shown. (C) The cells were seeded on Alexa Fluor 488–conjugated fibronectin (FN) for 24 h and then treated with or without Y27632 for another 6 h. The areas in which fibronectin had been degraded were measured. Data are expressed as fold relative to the level of v-Src–transformed FAK$^{-/-}$ MEFs in the absence of Y27632. #, $P < 0.05$. (D) The cells were subjected to a Matrigel invasion assay in the presence or absence of 10 µM Y27632. Data are expressed as fold relative to the level of v-Src–transformed FAK$^{-/-}$ MEFs in the absence of Y27632. (A, C, and D) Values (means ± SD) are from at least three independent experiments. (E) v-Src–transformed FAK$^{+/+}$ MEFs stably expressing mCherry-FAK and GFP-actin were monitored by time-lapse microscopy. Representative sequential images selected at different time points are shown. (F) v-Src–transformed FAK$^{+/+}$ MEFs stably expressing mCherry-FAK and GFP-actin were monitored by time-lapse microscopy in the presence or absence of 10 µM Y27632. The duration (means ± SD) of the disassembly phase in the total counted podosome rosettes ($n = 15$) was determined. (A, C, D, and F) *, $P < 0.005$.

(Fig. 9 A) and inhibited the formation of podosome rosettes (Fig. 9 C). Y27632 was able to reverse the effects of FAK depletion and RhoV14 on vimentin filaments and podosome rosettes (Fig. 9, A and C). More importantly, partial depletion of vimentin was able to compromise the defect in podosome rosette formation caused by FAK depletion or TAT-RhoV14 addition

(Fig. 9, B and C). Besides, in CL1-5 cells, the effects of FAK depletion and RhoV14 on vimentin filaments and podosome rosettes were confirmed in Src-transformed MEFs (Fig. S4). Together, these results suggest that FAK may facilitate the assembly of podosome rosettes through its suppression of Rho/ROCK signaling and vimentin filaments.
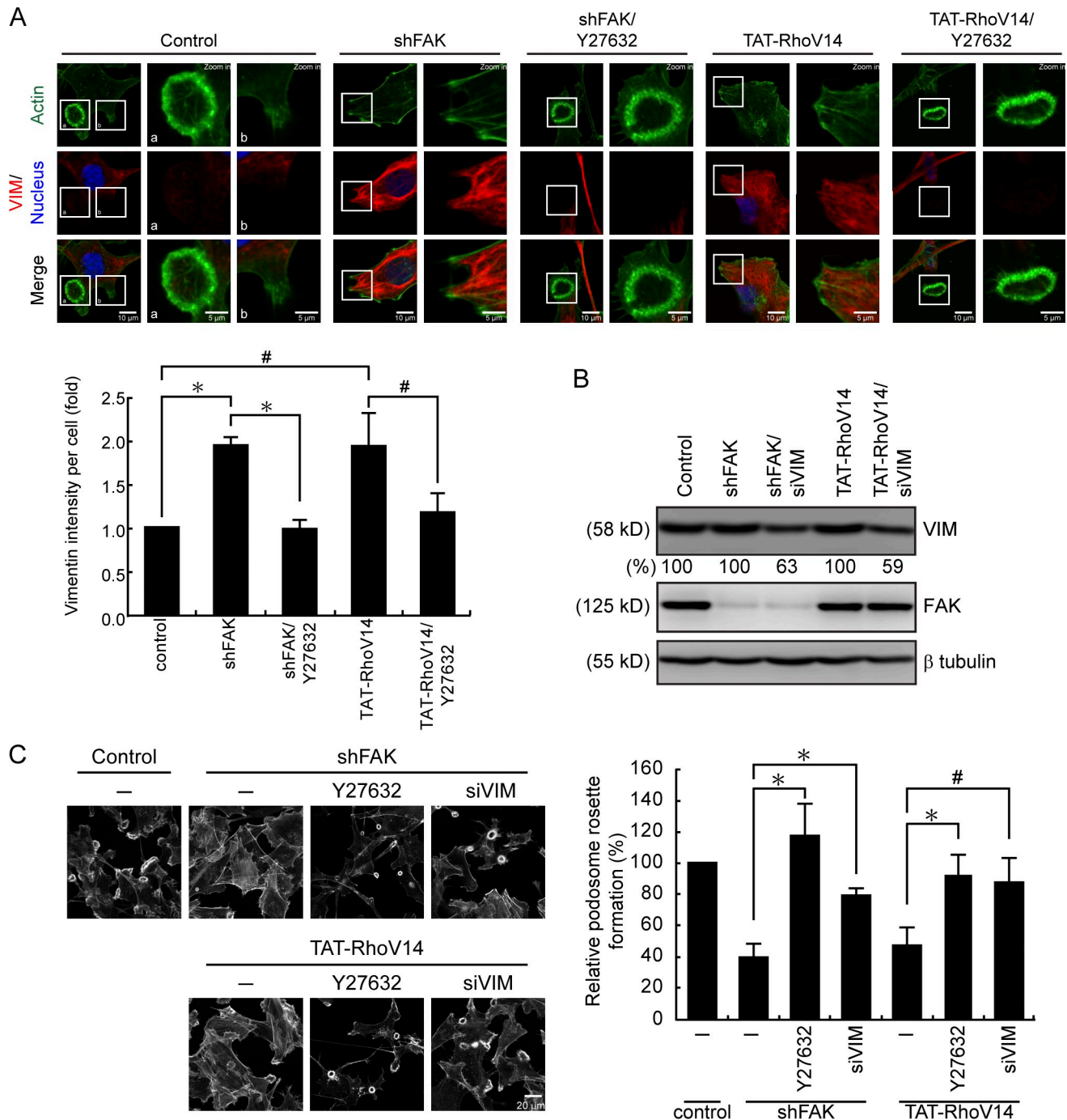
Figure 9. **Suppression of vimentin filaments by FAK facilitates the assembly of podosome rosettes.** (A) shRNAs specific to FAK (shFAK) or luciferase as a control were stably expressed in CL1-5 cells. The control cells were treated with 1 µg/ml TAT-RhoV14 for 12 h. In some cases, the cells were further treated with 10 µM Y27632. The cells were stained for F-actin, vimentin (VIM), and nuclei. The boxed areas from the images are enlarged. For the control cells, enlarged images from a podosome rosette (a) and the cell periphery (b) are shown. The fluorescent intensity of vimentin filaments per cell was measured (n = 30) and expressed as fold relative to the level of the control cells. (B) The CL1-5 cells expressing shFAK were transfected with duplex siRNA specific to vimentin (shFAK/siVIM). After 3 d, CL1-5 cells and those transfected with vimentin siRNA were treated with 1 µg/ml TAT-RhoV14 for 12 h. The expression of FAK and vimentin was analyzed by immunoblotting. (C) The cells were stained for F-actin. The formation of podosome rosettes was quantified. Values (means ± SD) are from three independent experiments. (A and C) *, $P < 0.005$; #, $P < 0.05$.

S39 and S72 of vimentin have been reported to be the phosphorylation sites for ROCK (Goto et al., 1998). We found that the filament structure of vimentin S39D or S72D mutant was more apparent than that of vimentin S39A or S72A mutant (Fig. 10 B), suggesting that ROCK-mediated phosphorylation of vimentin may facilitate its polymerization. Moreover, partial depletion of vimentin significantly increased the assembly of podosome rosettes in Src-transformed MEFs, which was reversed by reexpression of mCherry fluorescent protein–fused vimentin (cherry-VIM; Fig. 10 C). Notably, the S39A and S72A mutants were less potent than the S39D and S72D mutants in suppressing podosome rosettes (Fig. 10 C), indicating that less

polymerization of vimentin is inversely correlated with more podosome rosette formation. Moreover, the NH2-terminal fragment (aa 1–138) of vimentin that functions as a dominant-negative mutant (Chang et al., 2009) disrupted vimentin filaments (Fig. 10 D) and facilitated the formation of podosome rosettes (Fig. 10 E). Collectively, our results suggest that enhanced phosphorylation and polymerization of vimentin by ROCK may antagonize the assembly of podosome rosettes.

## Discussion

Podosomes can self-organize into large rosettelike structures in some types of cells. However, the mechanism of how this self-assembly is triggered remains largely unknown. In this study, we identified FAK as a key molecule necessary for the induction of podosome rosette assembly. Our results to support this conclusion are as follows: first, depletion of FAK suppressed the formation of podosome rosettes in Src-transformed fibroblasts, endothelial cells, carcinoma cells, and osteoclasts (Figs. 1 and S2). Second, oncogenic Src induced the formation of podosome rosettes only in FAK$^{+/+}$ MEFs but not in FAK$^{-/-}$ MEFs (Fig. 2). Third, dot-shaped podosomes were allowed to assemble into podosome rosettes only upon induction of FAK expression in Src-transformed FAK$^{-/-}$ MEFs (Figs. 3 and 5). Finally, in the absence of FAK, increased numbers of dot-shaped podosomes by the ROCK inhibitor Y27632 did not spontaneously trigger the assembly of podosome rosettes (Fig. 8). All of these results support a critical role for FAK in the assembly of podosome rosettes.

The formation of podosome belts is necessary for osteoclasts to perform bone resorption (Boyle et al., 2003). PYK2, the other member of the FAK family, has been reported to be essential for podosome belt formation as well as for bone resorption in osteoclasts (Gil-Henn et al., 2007). In this study, we demonstrated that depletion of FAK prevents the cluster-to-ring transition of podosomal organization in osteoclasts, whereas depletion of PYK2 prevents the ring-to-belt transition of podosomal organization in the cells (Fig. 1, H and I). These results suggest that FAK and PYK2 may coordinately regulate different stages of podosomal organization in osteoclasts. As the cluster-to-ring transition of podosomal organization in osteoclasts is somewhat analogous to podosome rosette assembly in other types of cells, the results derived from osteoclasts also support a critical role for FAK in podosome rosette assembly. However, what is the role of PYK2 in podosome rosette assembly in cells other than osteoclasts? It is apparent that PYK2 is not able to compensate the function of FAK for podosome rosette assembly in MEFs and CL1-5 cells, both of which express high levels of endogenous FAK and PYK2 (Fig. 1). In addition, although PYK2 is hardly detected in NIH3T3 fibroblasts and HUVECs, podosome rosettes can be formed in both types of cells (Figs. 1 and S2). Thus, our data suggest that FAK, but not PYK2, is crucial for podosome rosette assembly in fibroblasts, endothelial cells, and carcinoma cells.

Podosomes/invadopodia are commonly formed in cancer cells, whereas podosome rosettes appear to be assembled only in some highly invasive cancer cells such as breast cancer BT549 cells (Seals et al., 2005), melanoma RPMI-7951 cells (Seals et al., 2005), pancreatic carcinoma PaCa3 cells (Kocher et al., 2009), and lung adenocarcinoma cells such as CL1-5 cells (this study) and A549 cells (unpublished data). Our results clearly indicate that podosome rosettes are much more potent than dot-shaped podosomes to degrade ECM proteins (Figs. 2, 5, and 8). In addition, elevated expression of FAK is correlated with increases in podosome rosette formation, ECM degradation, and Matrigel invasion (Figs. 3 and 5). Conversely, FAK depletion is concomitant with decreases in podosome rosette formation, ECM degradation, and Matrigel invasion (Figs. 1, 2, and S2). Therefore, our data strongly suggest a link between FAK, podosome rosettes, and tumor invasion, which may explain, at least in part, why FAK plays an important role in tumor progression to a more malignant phenotype (McLean et al., 2005).

In this study, we demonstrated that v-Src induces dot-shaped podosomes both in FAK$^{-/-}$ MEFs and FAK$^{+/+}$ MEFs to a similar extent (Fig. 2), thus supporting that FAK is dispensable for dot-shaped podosomes, which is in agreement with recent studies describing that FAK is not necessary for the formation of invadopodia in breast cancer cells and colon cancer cells (Vitale et al., 2008; Chan et al., 2009). In contrast, Alexander et al. (2008) reported that FAK is present in invadopodia and is essential for invadopodia activity. In this study, we observed that FAK is associated with some, but not all, dot-shaped podosomes in Src-transformed MEFs (Fig. 4). Our findings could reconcile the discrepancy among previous studies that argue whether or not FAK is present in invadopodia (Alexander et al., 2008; Vitale et al., 2008; Chan et al., 2009). More importantly, we demonstrate that the dot-shaped podosomes with FAK association are more potent than those without FAK association for ECM degradation (Fig. 4, E and F). However, it is not clear whether dot-shaped podosomes with or without FAK association represent two different stages during the maturation of podosomes or two different subgroups of podosomes with different fates.

As the catalytic activity of FAK is important for its function in promoting podosome rosettes, it is possible that phosphorylation of certain FAK-interacting proteins by FAK may be important for podosome rosette assembly. In accordance with this idea, we found that the tyrosine phosphorylation of p130Cas is selectively regulated by FAK in Src-transformed MEFs, correlating with the formation of podosome rosettes in the cells (Fig. 6 C). In addition, the FAK mutant defective in p130Cas binding is less potent than wt FAK to restore podosome rosettes in Src-transformed FAK$^{-/-}$ MEFs (Fig. 6 B). Together, these results indicate that the interaction between FAK and p130Cas is important for the induction and/or maintenance of podosome rosettes. In fact, p130Cas and its tyrosine phosphorylation have been reported to be essential for the formation of podosome rosettes (Brábek et al., 2005) and invadopodia (Alexander et al., 2008).

In this study, we demonstrated that FAK promotes the formation of podosome rosettes in part through its suppression of Rho and ROCK in Src-transformed fibroblasts (Figs. 7 and 8). Activation of the Rho–ROCK signaling pathway has been
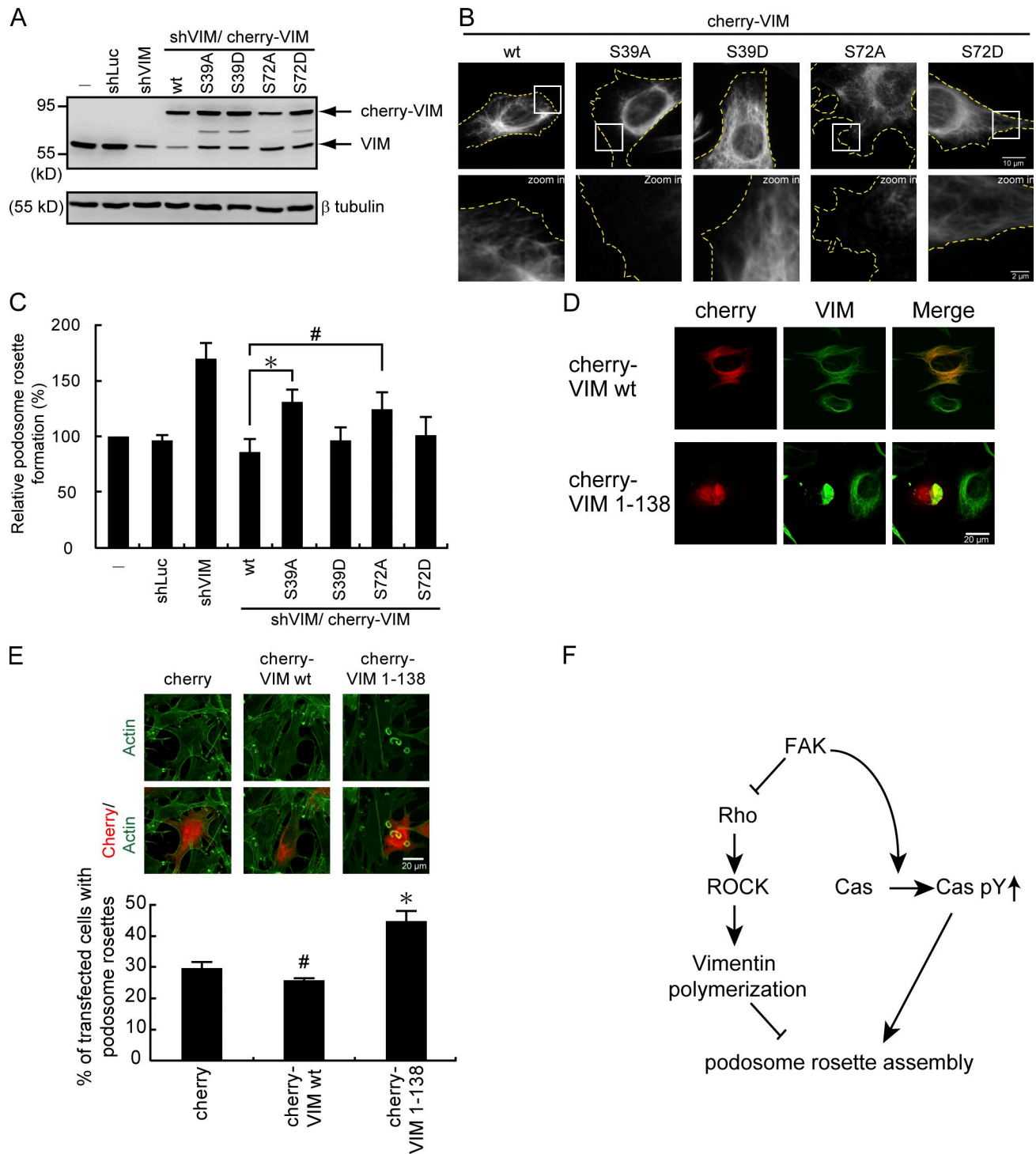
Figure 10. **Phosphorylation and polymerization of vimentin by ROCK antagonize the formation of podosome rosettes.** (A) Vimentin was depleted in v-Src–transformed FAK^{+/+} MEFs by shRNA (shVIM). Subsequently, mCherry-vimentin (cherry-VIM) or its mutants were stably reexpressed in the vimentin-depleted cells (shVIM/cherry-VIM). The expression of vimentin was analyzed by immunoblotting. (B) The organization of mCherry-vimentin in the cells was visualized under a fluorescent microscope (DM LB; Leica). The boxed areas from the images are enlarged. The yellow dashed lines mark the outlines of the cells. (C) The formation of podosome rosettes was measured and expressed as a percentage relative to the control cells. (D) mCherry-vimentin or its NH2-terminal fragment (aa 1–138) was transiently expressed in Src-transformed 3T3 cells. The cells were stained for vimentin. (E) The percentage of the cells containing podosome rosettes in the total counted cells expressing mCherry proteins ($n \geq 100$) was determined. (C and E) Values (means ± SD) are from three independent experiments. *, $P < 0.005$; #, $P < 0.05$. (F) A diagram illustrating that FAK may facilitate the assembly of podosome rosettes by promotion of p130Cas phosphorylation and suppression of the Rho-ROCK–vimentin pathway.

reported to promote actomyosin-based cell contraction and subsequent podosome dissolution (van Helden et al., 2008). Therefore, it is likely that activation of the Rho–ROCK signaling pathway may facilitate disassembly of podosome rosettes. In this study, we observed that the rosettelike structure of podosomes always becomes aggregated before it is completely dissolved (Fig. 8 E). This aggregation of F-actin might be because of the increased Rho/ROCK activity and actomyosin-based contraction at podosome rosettes. Consistent with this notion, we found that the ROCK inhibitor Y27632 significantly delayed the disassembly phase of podosome rosettes (Fig. 8 F). In osteoclasts, it has been shown that the formation of podosome belts is disrupted when the Rho activity is high (Destaing et al., 2005).

The dynamics of intermediate filaments can be regulated by Rho signaling (Inada et al., 1999). In this study, we surprisingly found that the organization of vimentin filaments is regulated by FAK in lung carcinoma CL1-5 cells (Fig. 9) and Src-transformed MEFs (Fig. S4). Depletion of FAK apparently enhances the organization of vimentin filaments in the cells, which is similar to the effect induced by active Rho. As FAK depletion and Rho activation have an adverse effect on the formation of podosome rosettes, our data thus suggest that enhanced organization of vimentin filaments may be disadvantageous to podosome rosettes. Indeed, fewer or no vimentin filaments are present in the surrounding areas of podosome rosettes (Fig. 9 A). Partial depletion of vimentin rescues the defect in the formation of podosome rosettes caused by FAK depletion or Rho activation (Fig. 9, B and C). Moreover, we found that the S39A and S72A mutants of vimentin are less organized into filaments and less potent in suppressing podosome rosettes than the S39D and S72D mutants (Fig. 10). Thus, our results suggest that enhanced phosphorylation and polymerization of vimentin by ROCK antagonize the formation of podosome rosettes. A recent study by Schoumacher et al. (2010) described that vimentin filaments penetrate invadopodia at a later stage of invadopodia maturation in carcinoma cells. However, it remains possible that the entry of vimentin filaments to invadopodia might be a mechanism for their disassembly.

In conclusion, we propose that although FAK is dispensable for the formation of dot-shaped podosomes/invadopodia, it is a key molecule necessary for the assembly of podosome rosettes. Tyrosine phosphorylation of p130Cas and suppression of Rho–ROCK signaling by FAK are important for the assembly. Finally, our results highlight that the infiltration of vimentin intermediate filaments may facilitate disassembly of podosome rosettes.

# Materials and methods

### Reagents
Polyclonal anti-FAK (A-17), anti-Cdc42, anticortactin (H-191), anti-Tks5 (M300), and anti–MT1-MMP (L-15) antibodies, monoclonal anti–β-tubulin (D-10) antibody, and duplex siRNA to vimentin were purchased from Santa Cruz Biotechnology, Inc. Monoclonal anti-FAK (clone 77), anti-p130Cas, anti-PYK2, antipaxillin, anti-p190RhoGAP, antiphosphotyrosine (PY20), anti-Rac1, and anti-RhoA antibodies and Matrigel were purchased from BD. Monoclonal antiacetylated tubulin (6-11B-1), anti-FLAG, antivinculin (clone hVIN-1), and antivimentin (clone V9 for immunofluorescent staining in human cells and clone VIM13.2 for immunofluorescent staining in mouse cells) antibodies, gelatin, nocodazole, and protein A–Sepharose beads

were purchased from Sigma-Aldrich. Polyclonal anti-MMP9 antibody, monoclonal anti-MMP2, and antivimentin (for immunoblotting) antibodies and collagen were purchased from Millipore. Polyclonal anti-PYK2 antibody was purchased from Cell Signaling Technology. Polyclonal anti–FAK pY577 and –Src pY416 antibodies were purchased from Invitrogen. The mouse ascites containing the monoclonal anti-Src (peptide 2–17) produced by hybridoma (CRL-2651) were prepared in our laboratory. Ni-nitrilotriacetic acid agarose beads and glutathione Sepharose 4B beads were purchased from GE Healthcare. Fibronectin, PMA, puromycin, hygromycin-B, and Y27632 were purchased from EMD. Lipofectamine and Oligofectamine were purchased from Invitrogen. FBS was purchased from Thermo Fisher Scientific.

### Plasmids
The plasmid pGEX-RANKL was provided by B. Lee (Ohio State University, Columbus, OH). The plasmid pKH3-FAK encoding HA-FAK was provided by J.L. Guan (University of Michigan, Ann Arbor, MI). The plasmids pEGFP-FAK and pEGFP-FAK-COOH domain were provided by D. Ilić (University of California, San Francisco, San Francisco, CA). The plasmids pTAT-His-TAT-RhoV14 and pTAT-His-TAT-C3 were provided by Z.F. Chang (National Yang-Ming University, Taipei, Taiwan). The plasmid pBabe-Hygro-p130Cas was provided by G.S. Goldberg (Stony Brook University, Stony Brook, NY). The plasmid pEGFP-N1-vimentin was provided by D. Lev (University of Texas M.D. Anderson Cancer Center, Houston, TX). The following plasmids were constructed in our laboratory: pEGFP-FAK-NH2 domain (aa 1–391); pmCherry-FAK; pKH3-FAK nt C1281A/A1284G (small hairpin RNA [shRNA]–resistant mutant); pLKO-AS2.puro-FLAG-FAK series including wt, Y397F, K454R, P712A/715A, P878A.881A, Y925F, ΔN (deletion of aa 1–374), and ΔC (deletion of aa 687–1,053); pEGFP-C2-p130Cas SH3 (aa 1–113); and pmCherry-vimentin series including wt, S39A, S39D, S72A, S72D, and N-terminal fragment (aa 1–138). All mutagenesis was performed using a QuikChange site-directed mutagenesis kit (Agilent Technologies), and the desired mutations were confirmed by dideoxy DNA sequencing.

### Cell culture and transfections
RAW264.7 cells purchased from the American Type Culture Collection were maintained in DME supplemented with 10% FBS. To induce differentiation of RAW264.7 cells into osteoclasts, RAW264.7 cells were seeded on glass coverslips coated with collagen for 24 h and were then treated with GST-RANKL at 100 ng/ml for 7 d. The multinucleated cells with an enlarged cell morphology were considered osteoclasts. HUVECs were prepared as previously described (Jaffe et al., 1973) and were maintained in M199 supplemented with low serum growth supplements (Invitrogen). FAK$^{+/+}$ MEFs and FAK$^{-/-}$ MEFs were obtained from D. Ilić and were maintained as previously described (Chen et al., 2002). Inducible Tet-FAK cells for FAK wt, Y397F, and Y576F/Y577F were obtained from S. Hanks (Vanderbilt University, Nashville, TN) and were maintained as previously described (Chang et al., 2005). To transform cells with v-Src, cells were transfected with pM–v-Src by Lipofectamine and selected by hygromycin. Lung adenocarcinoma CL1-5 cells were maintained as previously described (Chen and Chen, 2006). To knockdown vimentin in CL1-5 cells, CL1-5 cells were transfected with 66.7 nM duplex siRNA specific to vimentin by Oligofectamine. 3 d later, the cells were harvested for analysis.

### Lentiviral production and infection
The lentiviral expression system for shRNA was provided by the National RNAi Core Facility, Academia Sinica. For shRNA-mediated knockdown, the plasmids pLKO-AS1.puro encoding shRNAs were obtained from the National RNAi Core Facility, Academia Sinica. The target sequences for FAK are 5′-CCGGTCGAATGATAAGGTGTA-3′ (human #1), 5′-GCCCAG-GTTTACTGAACTTAA-3′ (human #2), 5′-GCCTTAACAATGCGTCAGTTT-3′ (mouse #1), and 5′-CGAGTATTAAAGGTCTTTCAT-3′ (mouse #2). The target sequences for PYK2 are 5′-CAAGGCTCTCTCATCATCCAT-3′ (human) and 5′-GCCTGTCCTTTACACACTCAT-3′ (mouse). The target sequence for p130Cas is 5′-CCTCAAGATTCTGGTTGGCAT-3′ (mouse). The target sequence for p190A is 5′-CTAAGGCTAGAGGCACTATTA-3′ (mouse). The target sequence for vimentin is 5′-GCTTCAAGACTCGGTGGACTT-3′ (mouse). For FAK expression, chicken FAK cDNA was amplified by a polymerase chain reaction and subcloned in frame to the NheI and AscI site of pLKO-AS2.puro-FLAG vector. To produce lentiviruses, HEK293T cells were cotransfected with 2.25 µg pCMV-ΔR8.91, 0.25 µg pMD.G, and 2.5 µg pLKO-AS1.puro-shRNA (or pLKO-AS2.puro-FLAG-FAK) by Lipofectamine. After 3 d, the medium containing lentivirus particles was collected and stored at −80°C. The cells were infected with recombinant lentiviruses in the presence of

8 µg/ml polybrene (Sigma-Aldrich) for 24 h. The cells were rinsed by DME and were allowed to grow in the growth medium for another 48 h. Subsequently, the cells were selected in the growth medium containing 0.5–2.5 µg/ml puromycin for 1 wk, and the puromycin-resistant cells were collected for analysis.

### Matrix degradation assay
Alexa Fluor 488–conjugated fibronectin and –conjugated gelatin were prepared according to the manufacturer's instructions (Invitrogen). Cells were plated on glass coverslips coated with 20 ng/ml Alexa Fluor 488–conjugated fibronectin or gelatin. After various durations, the cells were fixed and stained for F-actin and nuclei. The areas in which Alexa Fluor 488–conjugated matrix proteins were degraded were measured using Image-Pro Plus software (version 5.1; Media Cybernetics). A total of 10 random fields equivalent to 2 mm$^2$ was measured.

### Matrigel invasion assay
24-well transwell chambers (Costar) separated by a membrane with 8-µm pores were coated with 100 µl Matrigel (~2.7 mg/ml). The lower chamber was loaded with 750 µl DME with 10% serum. The cells were added to the upper chamber in 250 µl of serum-free medium. After 24 h, the cells that had migrated through the Matrigel were fixed by methanol, stained by Giemsa stain, and counted.

### Immunoprecipitation and immunoblotting
Immunoblotting and immunoprecipitation were performed as previously described (Chen and Chen, 2006). Chemiluminescent signals were detected and quantified using a luminescence image system (LAS-3000; Fujifilm).

### Small GTPase activity assay
GTP-bound RhoA in whole-cell lysates was pulled down by immobilized GST-Rhotekin–Ras-binding domain. GTP-bound Rac and Cdc42 in whole-cell lysates were pulled down by immobilized GST–p21-activated kinase–Ras-binding domain. The washed complexes were analyzed by immunoblotting with an antibody specific to RhoA, Rac1, or Cdc42.

### Purification of His-tagged TAT-RhoV14 and TAT-C3
His-tagged TAT fusion proteins were expressed in BL21 (DE3) *Escherichia coli* by isopropyl β-D-thiogalactopyranoside induction. The bacteria were lysed in lysis buffer (6 M Urea, 20 mM Tris, pH 7.9, 500 mM NaCl, and 5 mM imidazole), and His-tagged TAT fusion proteins were immobilized on Ni-nitrilotriacetic acid beads. The complexes were washed once with the lysis buffer and twice with washing buffer (20 mM Tris, pH 7.9, 500 mM NaCl, and 20 mM imidazole) and were then eluted by elution buffer (20 mM Tris, pH 7.9, 500 mM NaCl, and 1 M imidazole). The eluted proteins were dialyzed three times with 200 ml of 5% glycerol in PBS at 4°C for 15 min and stored at −80°C.

### Immunofluorescent staining and laser-scanning confocal fluorescent microscopy
For immunofluorescent staining, cells were fixed by 4% PFA in PBS for 30 min at room temperature and permeabilized with 0.05% Triton X-100 in PBS for 10 min at room temperature. To stain vimentin in mouse cells, cells were fixed by cold methanol for 10 min at −20°C and permeabilized with 0.05% Triton X-100 in PBS for 10 min at room temperature. The fixed cells were stained with primary antibodies at 4°C overnight followed by rhodamine- or Cy5-conjugated secondary antibodies (Invitrogen) for 3 h at room temperature. The primary antibodies used in immunofluorescent staining in this study were monoclonal antiacetylated tubulin (1:400), polyclonal anti-cortactin (1:200), polyclonal anti-FAK (1:200), polyclonal anti–Src pY416 (1:400), monoclonal anti-FAK (1:100), monoclonal antipaxillin (1:200), monoclonal antivinculin (1:200), and monoclonal antivimentin (clone V9 [1:400] and clone VIM13.2 [1:200]). rhodamine-conjugated phalloidin and Alexa Fluor 488–conjugated phalloidin (Invitrogen) were used to stain actin filaments. Coverslips were mounted in Anti-Fade DAPI-Fluoromount-G (SouthernBiotech) and viewed using a laser-scanning confocal microscope image system (LSM 510; Carl Zeiss) with a 63× Plan-Apochromat (NA 1.2 W Korr; Carl Zeiss) or a 100× Plan-Apochromat objective (NA 1.4 oil; Carl Zeiss).

### Time-lapse microscopy
v-Src–transformed FAK$^{+/+}$ cells that stably expressed mCherry-FAK and GFP-actin were grown on glass coverslips coated with 10 µg/ml fibronectin. The cells on the microscope stage were maintained at 37°C in a humid CO$_2$ atmosphere in a microcultivation system with temperature and CO$_2$ control devices (Carl Zeiss). The cells were monitored on an inverted microscope

(Axio Observer D1; Carl Zeiss) using a 63× Plan-Apochromat objective (NA 1.4 oil; Carl Zeiss). Images were captured every 2 min for 3 h using a digital camera (AxioCam MRm D; Carl Zeiss) and analyzed by Axio Vision Rel. software (version 4.8; Carl Zeiss). Wavelengths of 515–560 nm and 450–490 nm were used to excite mCherry and GFP. Beam path filters (beam paths 590–650 and 515–565 nm) were used to acquire images for the emission from mCherry and GFP.

### Statistics
Statistical analyses were performed by Student's *t* tests. Differences were considered to be statistically significant at $P < 0.05$.

### Online supplemental material
Fig. S1 shows that podosome rosettes protrude from the ventral surface of cells. Fig. S2 shows that FAK is crucial for podosome rosette formation in Src-transformed NIH3T3 cells and CL1-5 lung carcinoma cells. Fig. S3 shows that microtubules are not necessary for the formation of podosome rosettes in Src-transformed fibroblasts. Fig. S4 shows that FAK may promote podosome rosette formation by suppression of Rho signaling and vimentin filaments in Src-transformed MEFs. Online supplemental material is available at http://www.jcb.org/cgi/content/full/jcb.201103016/DC1.

## References

Alexander, N.R., K.M. Branch, A. Parekh, E.S. Clark, I.C. Iwueke, S.A. Guelcher, and A.M. Weaver. 2008. Extracellular matrix rigidity promotes invadopodia activity. *Curr. Biol.* 18:1295–1299. http://dx.doi.org/10.1016/j.cub.2008.07.090

Boyle, W.J., W.S. Simonet, and D.L. Lacey. 2003. Osteoclast differentiation and activation. *Nature.* 423:337–342. http://dx.doi.org/10.1038/nature01658

Brábek, J., S.S. Constancio, P.F. Siesser, N.Y. Shin, A. Pozzi, and S.K. Hanks. 2005. Crk-associated substrate tyrosine phosphorylation sites are critical for invasion and metastasis of SRC-transformed cells. *Mol. Cancer Res.* 3:307–315. http://dx.doi.org/10.1158/1541-7786.MCR-05-0015

Calalb, M.B., T.R. Polte, and S.K. Hanks. 1995. Tyrosine phosphorylation of focal adhesion kinase at sites in the catalytic domain regulates kinase activity: a role for Src family kinases. *Mol. Cell. Biol.* 15:954–963.

Cary, L.A., D.C. Han, T.R. Polte, S.K. Hanks, and J.L. Guan. 1998. Identification of p130Cas as a mediator of focal adhesion kinase-promoted cell migration. *J. Cell Biol.* 140:211–221. http://dx.doi.org/10.1083/jcb.140.1.211

Chan, K.T., C.L. Cortesio, and A. Huttenlocher. 2009. FAK alters invadopodia and focal adhesion composition and dynamics to regulate breast cancer invasion. *J. Cell Biol.* 185:357–370. http://dx.doi.org/10.1083/jcb.200809110

Chang, L.C., C.H. Huang, C.H. Cheng, B.H. Chen, and H.C. Chen. 2005. Differential effect of the focal adhesion kinase Y397F mutant on v-Src-stimulated cell invasion and tumor growth. *J. Biomed. Sci.* 12:571–585. http://dx.doi.org/10.1007/s11373-005-7212-5

Chang, L., K. Barlan, Y.H. Chou, B. Grin, M. Lakonishok, A.S. Serpinskaya, D.K. Shumaker, H. Herrmann, V.I. Gelfand, and R.D. Goldman. 2009. The dynamic properties of intermediate filaments during organelle transport. *J. Cell Sci.* 122:2914–2923. http://dx.doi.org/10.1242/jcs.046789

Chen, S.Y., and H.C. Chen. 2006. Direct interaction of focal adhesion kinase (FAK) with Met is required for FAK to promote hepatocyte growth factor-induced cell invasion. *Mol. Cell. Biol.* 26:5155–5167. http://dx.doi.org/10.1128/MCB.02186-05

Chen, B.H., J.T. Tzen, A.R. Bresnick, and H.C. Chen. 2002. Roles of Rho-associated kinase and myosin light chain kinase in morphological and migratory defects of focal adhesion kinase-null cells. *J. Biol. Chem.* 277:33857–33863. http://dx.doi.org/10.1074/jbc.M204429200

Chen, T.H., P.C. Chan, C.L. Chen, and H.C. Chen. 2011. Phosphorylation of focal adhesion kinase on tyrosine 194 by Met leads to its activation through relief of autoinhibition. *Oncogene.* 30:153–166. http://dx.doi.org/10.1038/onc.2010.398

Chen, W.T., J.M. Chen, S.J. Parsons, and J.T. Parsons. 1985. Local degradation of fibronectin at sites of expression of the transforming gene product pp60src. *Nature*. 316:156–158. http://dx.doi.org/10.1038/316156a0

Destaing, O., F. Saltel, J.C. Géminard, P. Jurdic, and F. Bard. 2003. Podosomes display actin turnover and dynamic self-organization in osteoclasts expressing actin-green fluorescent protein. *Mol. Biol. Cell*. 14:407–416. http://dx.doi.org/10.1091/mbc.E02-07-0389

Destaing, O., F. Saltel, B. Gilquin, A. Chabadel, S. Khochbin, S. Ory, and P. Jurdic. 2005. A novel Rho-mDia2-HDAC6 pathway controls podosome patterning through microtubule acetylation in osteoclasts. *J. Cell Sci.* 118:2901–2911. http://dx.doi.org/10.1242/jcs.02425

Gil-Henn, H., O. Destaing, N.A. Sims, K. Aoki, N. Alles, L. Neff, A. Sanjay, A. Bruzzaniti, P. De Camilli, R. Baron, and J. Schlessinger. 2007. Defective microtubule-dependent podosome organization in osteoclasts leads to increased bone density in *Pyk2*−/− mice. *J. Cell Biol.* 178:1053–1064. http://dx.doi.org/10.1083/jcb.200701148

Gimona, M., R. Buccione, S.A. Courtneidge, and S. Linder. 2008. Assembly and biological role of podosomes and invadopodia. *Curr. Opin. Cell Biol.* 20:235–241. http://dx.doi.org/10.1016/j.ceb.2008.01.005

Goto, H., H. Kosako, K. Tanabe, M. Yanagida, M. Sakurai, M. Amano, K. Kaibuchi, and M. Inagaki. 1998. Phosphorylation of vimentin by Rho-associated kinase at a unique amino-terminal site that is specifically phosphorylated during cytokinesis. *J. Biol. Chem.* 273:11728–11736. http://dx.doi.org/10.1074/jbc.273.19.11728

Guan, J.L., and D. Shalloway. 1992. Regulation of focal adhesion-associated protein tyrosine kinase by both cellular adhesion and oncogenic transformation. *Nature*. 358:690–692. http://dx.doi.org/10.1038/358690a0

Ilić, D., Y. Furuta, S. Kanazawa, N. Takeda, K. Sobue, N. Nakatsuji, S. Nomura, J. Fujimoto, M. Okada, and T. Yamamoto. 1995. Reduced cell motility and enhanced focal adhesion contact formation in cells from FAK-deficient mice. *Nature*. 377:539–544. http://dx.doi.org/10.1038/377539a0

Inada, H., H. Togashi, Y. Nakamura, K. Kaibuchi, K. Nagata, and M. Inagaki. 1999. Balance between activities of Rho kinase and type 1 protein phosphatase modulates turnover of phosphorylation and dynamics of desmin/vimentin filaments. *J. Biol. Chem.* 274:34932–34939. http://dx.doi.org/10.1074/jbc.274.49.34932

Jaffe, E.A., R.L. Nachman, C.G. Becker, and C.R. Minick. 1973. Culture of human endothelial cells derived from umbilical veins. Identification by morphologic and immunologic criteria. *J. Clin. Invest.* 52:2745–2756. http://dx.doi.org/10.1172/JCI107470

Kocher, H.M., J. Sandle, T.A. Mirza, N.F. Li, and I.R. Hart. 2009. Ezrin interacts with cortactin to form podosomal rosettes in pancreatic cancer cells. *Gut*. 58:271–284. http://dx.doi.org/10.1136/gut.2008.159871

Linder, S. 2007. The matrix corroded: podosomes and invadopodia in extracellular matrix degradation. *Trends Cell Biol.* 17:107–117. http://dx.doi.org/10.1016/j.tcb.2007.01.002

Linder, S., and M. Aepfelbacher. 2003. Podosomes: adhesion hot-spots of invasive cells. *Trends Cell Biol.* 13:376–385. http://dx.doi.org/10.1016/S0962-8924(03)00128-4

Luxenburg, C., D. Geblinger, E. Klein, K. Anderson, D. Hanein, B. Geiger, and L. Addadi. 2007. The architecture of the adhesive apparatus of cultured osteoclasts: from podosome formation to sealing zone assembly. *PLoS ONE*. 2:e179. http://dx.doi.org/10.1371/journal.pone.0000179

McLean, G.W., N.O. Carragher, E. Avizienyte, J. Evans, V.G. Brunton, and M.C. Frame. 2005. The role of focal-adhesion kinase in cancer - a new therapeutic opportunity. *Nat. Rev. Cancer*. 5:505–515. http://dx.doi.org/10.1038/nrc1647

Ren, X.D., W.B. Kiosses, D.J. Sieg, C.A. Otey, D.D. Schlaepfer, and M.A. Schwartz. 2000. Focal adhesion kinase suppresses Rho activity to promote focal adhesion turnover. *J. Cell Sci.* 113:3673–3678.

Schaller, M.D., J.D. Hildebrand, J.D. Shannon, J.W. Fox, R.R. Vines, and J.T. Parsons. 1994. Autophosphorylation of the focal adhesion kinase, pp125FAK, directs SH2-dependent binding of pp60src. *Mol. Cell. Biol.* 14:1680–1688.

Schlaepfer, D.D., S.K. Mitra, and D. Ilic. 2004. Control of motile and invasive cell phenotypes by focal adhesion kinase. *Biochim. Biophys. Acta*. 1692:77–102. http://dx.doi.org/10.1016/j.bbamcr.2004.04.008

Schoumacher, M., R.D. Goldman, D. Louvard, and D.M. Vignjevic. 2010. Actin, microtubules, and vimentin intermediate filaments cooperate for elongation of invadopodia. *J. Cell Biol.* 189:541–556. http://dx.doi.org/10.1083/jcb.200909113

Seals, D.F., E.F. Azucena Jr., I. Pass, L. Tesfay, R. Gordon, M. Woodrow, J.H. Resau, and S.A. Courtneidge. 2005. The adaptor protein Tks5/Fish is required for podosome formation and function, and for the protease-driven invasion of cancer cells. *Cancer Cell*. 7:155–165. http://dx.doi.org/10.1016/j.ccr.2005.01.006

Sieg, D.J., C.R. Hauck, D. Ilic, C.K. Klingbeil, E. Schaefer, C.H. Damsky, and D.D. Schlaepfer. 2000. FAK integrates growth-factor and integrin signals to promote cell migration. *Nat. Cell Biol.* 2:249–256. http://dx.doi.org/10.1038/35010517

Tatin, F., C. Varon, E. Génot, and V. Moreau. 2006. A signalling cascade involving PKC, Src and Cdc42 regulates podosome assembly in cultured endothelial cells in response to phorbol ester. *J. Cell Sci.* 119:769–781. http://dx.doi.org/10.1242/jcs.02787

van Helden, S.F., M.M. Oud, B. Joosten, N. Peterse, C.G. Figdor, and F.N. van Leeuwen. 2008. PGE2-mediated podosome loss in dendritic cells is dependent on actomyosin contraction downstream of the RhoA-Rho-kinase axis. *J. Cell Sci.* 121:1096–1106. http://dx.doi.org/10.1242/jcs.020289

Vitale, S., E. Avizienyte, V.G. Brunton, and M.C. Frame. 2008. Focal adhesion kinase is not required for Src-induced formation of invadopodia in KM12C colon cancer cells and can interfere with their assembly. *Eur. J. Cell Biol.* 87:569–579. http://dx.doi.org/10.1016/j.ejcb.2008.04.002